



● *Original Contribution*

**ULTRASOUND AND MICROBUBBLES: THEIR GENERATION,
 DETECTION AND POTENTIAL UTILIZATION IN TISSUE AND
 ORGAN THERAPY—EXPERIMENTAL**

FRANCIS J. FRY,[†] NARENDRA T. SANGHVI,[‡] RICHARD S. FOSTER,*
 RICHARD BIHRLE* and CARL HENNIGE[§]

[†]Indianapolis Center for Advanced Research, VanNuys Medical Science Building, Indianapolis, IN, USA;
[‡]Departments of [§]Physiology and Biophysics and ^{*}Urology, Indiana University School of Medicine,
 Indianapolis, IN, USA; and [§]Focus Surgery Inc., Milpitas, CA, USA

(Received 23 August 1994; in final form 10 April 1995)

Abstract—Ultrasound-induced cavitation in tissue and organs has been well recognized and documented. Generally, this phenomenon has been seen as something to be avoided except in cases such as lithotripsy, where its production is considered an essential part of the treatment process or as a desirable contrast media in some areas of visualization enhancement. This article covers three areas in which the phenomenon has been observed, and shows how the effect can or may be therapeutically beneficial. Studies in the pig show that implanted human gallstones and the gallbladder itself can be eliminated in a nonsurgical procedure using ultrasound-induced cavitation in the gallbladder. In the dog brain, relatively stable cavitation-induced microbubbles have been transported through the vascular system to regions outside a focal seeding site. These bubbles produce ablation of tissue volumes at a remote site when irradiated with appropriate ultrasound. The cavitation phenomenon has been observed in the dog and human prostate. In the human prostate, microbubbles transported from ultrasound-induced focal seeding sites can be readily visualized with ultrasound and may be potentially useful under controlled conditions in tissue debulking for the treatment of benign prostatic hyperplasia (BPH). A similar microbubble transport has not been seen in the dog prostate under similar ultrasound treatment parameters. The ability to detect cavitation-induced microbubbles, follow their transportation through the vascular system and excite them at the appropriate time and place provides interesting possibilities for therapy. Of course, the entire microbubble process can be avoided by working below the cavitation threshold, thereby using only the absorption of ultrasound in tissue to produce focal thermal lesions. The term microbubble is used here in the context of those bubbles which can be transported in the vascular system down to vessels diameters below the 100- μ m range. This is the vessel size in the vascular field into which microbubbles are transported and can be both visualized as well as disrupted with ultrasound.

Key Words: Ultrasound, Microbubbles, Cavitation, Tissue and organ therapy.

INTRODUCTION

Cavitation microbubble production in fluids under ultrasound exposure was one of the earliest phenomena observed and studied (Apfel 1981; Benjamin and Ellis 1966; Blake 1949; Crum and Fowlkes 1986; Eller and Flynn 1969; Esche 1952; Flynn 1975; Jones and Edwards 1960; Neppiras 1968; Noltingk and Neppiras 1950). Of interest here is the production and occurrence of cavitation phenomena *in vivo* under ultrasound exposure. This effect is of major interest because of

its potential impact in diagnostic and therapeutic ultrasound applications.

When gaseous inclusions are a part of the living system cavitation effects can be readily elicited (Child et al. 1981; O'Brien and Zachary 1994; Tarantal and Canfield 1994). Without gaseous inclusions, as is the case for mammalian tissues of interest here, the production and detection of cavitation microbubbles has required more elaborate procedures, but there is emerging a body of data identifying cavitation irradiation thresholds for intact living tissue (Chapelon et al. 1992; Fowlkes et al. 1994; Frizzell et al. 1983; Hynynen 1991; Lele 1978; Sommer and Pounds 1982; ter Haar et al. 1982).

Address correspondence to: Narendra T. Sanghvi, Indianapolis Center for Advanced Research, VanNuys Medical Science Building, Indianapolis, IN 46202, USA.

Gallbladder and gallstones

For studies on gallstone dissolution using cavitation enhancement as a potential therapeutic method it was necessary to establish, through *in vitro* studies, that physiologically acceptable fluids were suitable for the process. In addition, it was necessary to identify an optimal ultrasound frequency for the dissolution rate process while maintaining an ultrasound intensity which would not damage tissues in the sound transmission path from the external skin surface to the gallbladder and beyond. In this case a deliberate attempt was made to maximize the cavitating effects between the ultrasound field and the immersed gallstones. The ultimate experimental animal test was the *in vivo* study with human gallstones surgically implanted in the pig gallbladder. These tests were used to maximize the stone dissolution rate within the bounds of tissue safety required for any subsequent human therapeutic implementation.

Brain

Studies in the production of large volume lesions from a multiplicity of individual focal lesions in the adult dog brain provide the basis for focal cavitation microbubble seeding sites. These microbubbles are transported in the vascular system to remote sites, which if they fall in very much reduced intensity regions of the sound field path, may violently collapse and produce large hemorrhagic tissue volumes consistent with the microbubble-embedded regions in the vascular system. In single-lesion site studies for the identification of focal tissue destruction thresholds as a function of sound intensity, this microbubble transport phenomena has not been reported since there was no follow-up of tissue observation using ultrasound visualization, nor was there a subsequent irradiation process, which is needed to initiate lesion production remote to the single site sound focus. Cavitation effects as a result of single site focal placement of the sound have been histologically documented (Fry et al. 1970). The fullest revelation of microbubble seeding in and subsequent transport through the vasculature system in brain was seen when volume lesions in gray matter were attempted at a 1-MHz frequency (Fry 1993). These volume lesions were produced by multiple-site placement of individual focal lesions. Previous studies in which this seeding was not observed were based on volume lesions at a 1-MHz frequency in brain white matter where lesions are readily produced from multiple-site individual focal lesions at well below the cavitation threshold (Fry and Meyers 1962). When volume lesions were produced in gray matter of experimental animal brains the frequency used was 4 MHz, which has a substantially higher intensity threshold for cavitation than does 1-MHz ultrasound. Here again the microbubble transport

phenomena was not observed, at least as evidenced by no lesions produced outside the intended focal site and the ability to continue to produce lesions at the intended focal depth without any diminution in capability. (Fry and Meyers 1962). These data along with other information (Hynynen 1991) support the concept that *in vivo* the cavitation threshold does increase with frequency in a number of cases.

Prostate

Studies in the production of large volume lesions in the live dog prostate using a multiplicity of single site focal lesions at 4 MHz show the transition from non-gaseous inclusion sites to those which produce a gaseous inclusion (vapor phase in the tissue). In the dog prostate, the presumed production of microbubbles at seeding sites coincident with the gaseous inclusion does not appear to provide a basis for subsequent lesion production and hemorrhage outside the primary focal site; that is, there is no physical evidence (ultrasound visualization) for vascular transport of microbubbles. In the human prostate being treated for BPH the case may be considerably different. Once cavitation microbubble production has occurred at the primary focal site there is a considerable possibility that these microbubbles will be transported by the vascular system to remote sites in the prostate as seen on ultrasound visualization leading to the possibility of lesion production at sites in the near field sound pathway which are of a considerably reduced sound field intensity. This difference in response between the dog and human is not understood at present.

MATERIALS AND METHODS

Gallbladder and gallstones

The *in vitro* studies on gallstone dissolution were conducted in a 37°C degassed water bath where a thin latex envelope (surgeon's glove finger) was suspended in which the human gallstones and the selected immersion fluids were contained.

A broad beam at 220 kHz, generated by a 7.5-cm-diameter piezoceramic transducer was used for the irradiation under continuous-wave (CW) burst mode (4 s time on, 20 s time off for a total irradiation time of 20 min) conditions. Most of the pertinent data have been reported elsewhere (Griffith et al. 1990). Additional information previously reported involved irradiation under increased pressure (Sanghvi et al. 1990). These studies were conducted in a hyperbaric chamber.

The gallstones studied were primarily the cholesterol type and the immersion fluids were water, bile, monoocetanol and MTBE (methyl-tertiary-butyl ether). To determine the dissolution rate the stones were weighed at preirradiation and at fixed time intervals thereafter de-

pending on the fluid involved and the sound field intensity used.

Selection of the frequency for irradiation was based on dissolution studies at frequencies of 100, 220, 500 and 1000 kHz. Calibration of the sound field intensity was done with a stainless-steel ball radiometer.

All *in vivo* studies involved the young pig (40 to 50 kg in weight). Selected human gallstones were surgically implanted in the pig gallbladder under sterile conditions. After initial sedation irradiation under gaseous anesthesia (5% Halothane) was conducted generally at 2 weeks after stone implantation. For the initial studies the pig was suspended in a supine position in a degassed 37°C water bath (Griffith *et al.* 1990). The skin surface was prepared using a depilatory followed by soap scrubbing and alcohol rinsing. A specially designed 4-French catheter was inserted transcutaneously into the gallbladder under real-time ultrasound guidance. Bile was withdrawn under ultrasound observation and the immersion fluid of a volume equal to the bile withdrawn was inserted. Careful attention was made to exclude gas at injection, but this could have occurred. It was presumed that any such gas introduced was of little consequence since no bubbles showed on real-time scans taken during the time of filling. Alignment of the irradiating transducer was done using a pointer attached to the transducer which defined the beam center radially and established the transducer to skin distance. Marks on the skin were used to identify the entry window and the angulation of the transducer which was the same in all cases. The sound was delivered in the CW burst mode described above with the irradiation time extended to 97 min. After the ultrasound procedures, the fluid was withdrawn from the gallbladder which was then flushed gently with sterile saline. Thermocouples in the pig gallbladder showed a maximum temperature rise of 5°C with the highest intensity used (8 W cm⁻² SPTP) in the animal studies. Extensive blood chemistry studies were conducted throughout the course of the pigs' survival.

Irradiated animals and control animals were killed at intervals ranging from acute to 2, 4 and 6 weeks after therapy procedure. At autopsy visual observation was made of the gallbladder and all tissues starting from the animal skin entry through the skin exit area. Histological studies were performed on the entire gallbladder and any other tissue which showed deviation from normal appearance (Griffith *et al.* 1990), as seen at autopsy. A pathologist scored all the slides and tissue samples.

For a human clinical study (FDA, Phase I), a new system was designed and built, utilizing the basic information acquired from the laboratory animal study (Sanghvi *et al.* 1990). This new system did not include a water bath (as was used in the initial animal studies)

and utilized a couch with a back-ultrasound absorber coupled to the subject to prevent any exit injury on the skin. The non-water bath system was very useful in establishing the sound intensity with gel coupling, which in the human could produce undesirable pain levels. Water coupling raised the sound intensity level at which pain occurred at the skin.

Brain

The brain lesioning study used the dog as the experimental animal. The anesthetized animal was mounted in a skull fixation apparatus as previously described (Fry and Dunn 1962) and a 3 cm × 3 cm section of the calvarium removed. A coupling pan containing degassed mammalian Ringer solution was attached via a tourniquet to the scalp skin and the transducer, appropriately located in the fluid, produced the focused beam which transversed the fluid to the brain sites selected for lesioning. The focus of the sound beam was placed in the lateral thalamic region approximately 1.0 cm below the dura surface and 0.5 cm lateral to the midline at a position 1.0 cm anterior to the ear bar zero of the skull fixation apparatus. This placed the beam focus in gray matter and mixed white and gray matter. All these procedures have been described elsewhere (Fry and Dunn 1962). Since the system designed and constructed for these studies was to be used for human clinical studies the frequencies available were 1 and 3 MHz to have a full range of brain depth penetration. The entire system has been described elsewhere (Fry *et al.* 1986). For volume lesion production two series of individual focal lesions were placed 2 mm apart laterally to provide a 1-cm lateral sized lesion and 2 mm apart longitudinally to provide a 1-cm longitudinal lesion. Real-time ultrasound was used to scan the brain after each individual lesion was placed. Depending on the results of the ultrasound scans the irradiation was terminated as echoes appeared from outside the focal site. The animal was perfused, and the brain removed and sectioned for direct observation. Once the cavitation threshold was determined by the above method the full focal site lesion volume was produced by working below the cavitation threshold using a multiplicity of individual site lesions. These brains were removed and prepared by established histological procedures and the size and shape of the lesion determined by measurement from the stained slide sections.

Prostate

A transrectal focused ultrasound probe operating at 4 MHz was used to produce volume lesions in the dog prostate. The same transducer element used for lesion production was also used for visualization. The visualization scan rate was four cycles per second. This system has been described elsewhere (Sanghvi *et al.*

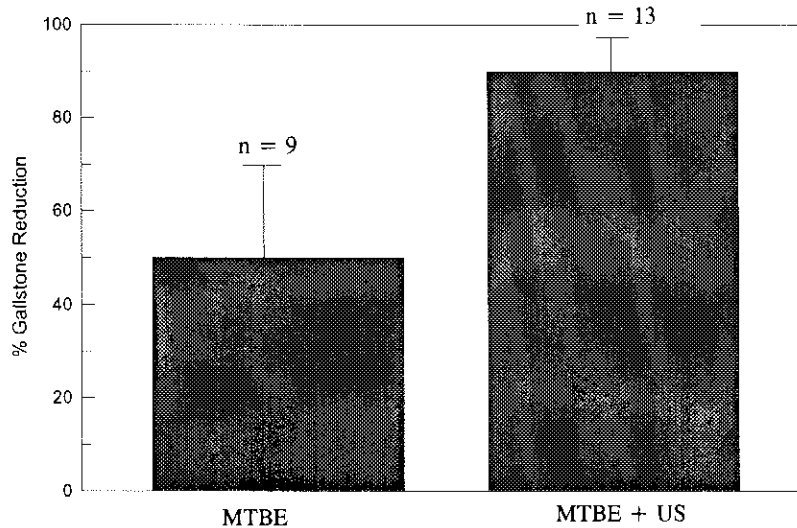


Fig. 1. *In vivo* results with MTBE and MTBE+ ultrasound (US). The MTBE+ ultrasound reduction is significant at $p < 0.001$.

1992). Focal intensities in the prostate were varied from 700 to 2000 W cm^{-2} (spatial peak, temporal peak, SPTP) and irradiation times per single site varied from 12 s at the lowest intensity to 4 s at the highest intensity. A volume lesion was produced by spacing the individual site lesions 2 mm apart in both the longitudinal and the lateral direction. A visualization update was made after each individual site exposure. This permits observation of any echo changes in the image as a result of the sound irradiation. All of the visualization information was recorded for subsequent evaluation. Depending on the nature of the study, animals were killed by lethal injection of euthanasia solution either acute or at 1, 2, 4, 8 or 12 weeks subsequent to irradiation. The animals were perfused with 10% formalin after killing, and the prostate and surrounding tissues (bladder and rectum) removed for gross observation with subsequent histology (Foster et al. 1993).

In human subjects treated for BPH the same system was used (Bihrlé et al. 1994). In these cases, there was of course no histological follow-up. After each individual lesion placement the scanning mode was activated and both echo changes at the focal site and outside this site in the prostate were recorded. The echo patterns were analyzed for their relevance in terms of microbubble production and transport in the vascular system within the prostate.

All animal experiment were carried out in accordance to the protocol approved by the Indiana University Campus Animal Resource Committee.

RESULTS

Gallbladder and gallstones

Cholesterol gallstone erosion *in vivo* using MTBE (Fig. 1) and 3 W cm^{-2} (SPTP in the burst mode de-

scribed above and applied for 97 min) of 220-kHz ultrasound follows a pattern that is typical for the *in vitro* case. The control erosion without ultrasound is also shown. When erosion is studied *in vitro* under pressure the results are shown in Fig. 2. The intensity used with 3 W cm^{-2} SPTP applied for 35 min in the burst mode described above.

When cholesterol gallstone erosion rate was studied with MTBE and ultrasound as a function of frequency the results showed a maximum erosion rate in the 220-kHz range.

In vivo results of stone erosion with MTBE and ultrasound are shown in Table 1. Above an intensity of 3 W cm^{-2} with MTBE there is an effect on the gallbladder itself which indicates the possibility for total gallbladder atrophy (7 of 10 pigs killed at 1 week or later demonstrated some degree of gallbladder ablation). This amounted to the formation of a fibrotic mass of scar tissue with no lumen, no mucosa and a patent cystic duct. In two pigs killed at 1 year postirradiation one had no gallbladder in evidence and the other had a small fibrous remnant with some evidence of gallbladder regeneration.

The FDA approved protocol in a limited human series with MTBE and ultrasound eliminated the use of ultrasound in eight cases (the stone erosion rate was adequate with MTBE alone). Previous clinical studies report gallstone erosion with MTBE (May and Thistle 1986). Based in part on these studies the human protocol called for ultrasound application only if the measured gallstone erosion was inadequate as determined by ultrasound scans. In the two cases in which ultrasound was administered, the applied intensity of 4 W cm^{-2} showed an increase in one case of the erosion rate from that expected from MTBE alone. The level

Table 1. *In vivo* treatment group (MTBE and ultrasound).

Fig. no.	Total weight of stones (mg)	Posttreatment time (weeks)	Stone reduction	
			Milligrams	Percent
1	539	0	446	82.7
2	536	0	536	100.0
3	518	0	446	86.1
4	513	1	400	78.0
5	495	2	495	100.0
6	502	2	502	100.0
7	524	2	380	72.5
8	551	4	551	100.0
9	505	4	497	98.4
10	514	4	514	100.0
11	491	6	491	100.0
12	506	6	356	70.4
13	502	6	502	100.0

Averages \pm 1.0 SD for various parameters of interest: number of stones implanted, 3.5 ± 2 ; total weight of stones, $515.08 \text{ mg} \pm 18.03 \text{ mg}$; absolute stone reduction (mg), $470.46 \pm 60.44 \text{ mg}$; percentage stone reduction, $91.39\% \pm 11.71\%$. Sound applied in the burst mode described in the text at 3 W cm^{-2} SPTP for 97 min total elapsed time.

of intensity was limited by two factors. One was the desire to stay below a level (approximately 3 to 4 W cm^{-2}) which showed gallbladder effects in the pig. The other consideration was limited by the patient's complaint of skin pain in the gel-coupled region of the applicator. This pain threshold occurred just above 4 W cm^{-2} .

The result of degassed water coupling with the applicator indicated that an intensity of 12 W cm^{-2} could be achieved at the human skin surface without related pain. In any further studies using this method the water coupling will provide considerably more latitude for the ultrasound intensity parameter.

Brain

At 1 MHz and a focal intensity of 750 W cm^{-2} (SPTP) in the dog brain (thalamic region) there was always a hemorrhagic effect produced at the cortical gray and subcortical white matter interface region in the hemisphere being irradiated when multiple adjacent focal sites were exposed to ultrasound. This hemorrhage was readily observed with real-time ultrasound scanning which was performed after each focal site was exposed. It could also be visually observed as a bluish darkening of the cortical region through the clear Ringer solution in the coupling pan. The effect was never observed after the first exposure, but was seen after some subsequent exposure and was always seen by at least the fifth exposure. This effect was produced along the entry path of the sound beam approximately 10 mm above the focal site in a very much reduced intensity region of the sound field. A schematic representation of this sequence is shown in Fig. 3. Once this hemorrhagic event occurred it was not possible to continue to produce focal lesions at the deeper intended site. The flow of blood in brain courses from the basal aspect in a cortical direction, and at the brain position of the focal lesions in this study there is no blood flow crossover into the opposite hemisphere. This vascular feature was nicely demonstrated as a microbubble restricting barrier in that the hemorrhagic overlay was restricted to the hemisphere being focally irradiated even though, at the brain position of the hemorrhagic site, portions of the opposite hemisphere were in the sound field entry path receiving equal sound intensity. Although Fig. 3 does not fully display the focal lesion sites when the focus was moved toward the brain midline the beam entry pattern for the near midline lesions encompassed the hemisphere not focally irradiated.

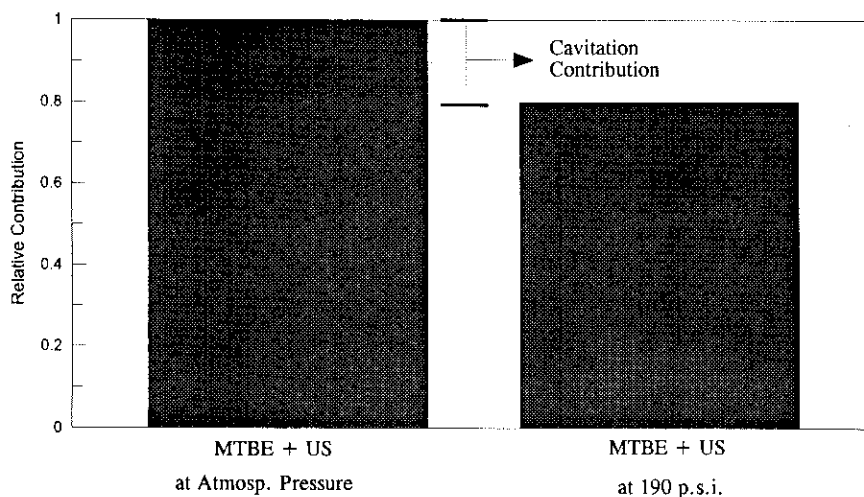


Fig. 2. Relative contribution of cavitation to gallstone weight reduction in MTBE with ultrasound (US) applied for 35 min *in vitro*.

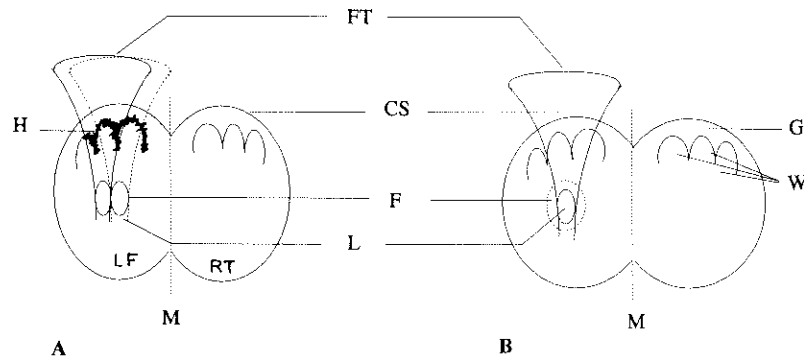


Fig. 3. Coronal section of dog brain. FT = focused transducer; CS = cortical surface; H = hemorrhage; F = focus of beam; L = lesion; G = gray matter; W = white matter of brain; M = brain midline; LF = left brain side; RT = right brain side. (a) Multiple-site lesion leading to bubble seeding emanating from the focal lesion site. These bubbles are transported by the blood vessels to the gray–white matter interfaces indicated and on subsequent irradiation hemorrhage results as shown. This hemorrhage is restricted to the left brain (LF) and does not show in the right brain (RT), since there is no brain hemisphere crossover of blood flow in this region. (b) Single-site lesion. Expanded lesion volume (---) is produced by multiple exposure at a single site which does not produce hemorrhagic overlay.

When a single site was focally irradiated up to 10 times this hemorrhagic effect could not be produced, which indicated an apparent need for movement of the cavitation microbubble seeding sites to elicit the full-blown effect. When the focal intensity was reduced below 400 W cm^{-2} this effect never occurred and multiple focal thermal lesions were used to produce complex lesion volumes such as those shown in Fig. 4. The complete volume lesion of which Fig. 4 shows only one cross-section required 50 individual single site focal lesion placements. At a frequency of 4 MHz and

an intensity of 1000 W cm^{-2} , volume lesions in brain can be produced without this overly hemorrhagic effect (Fry and Meyers 1962).

Prostate

Irradiation of the dog prostate at 4 MHz and a focal site intensity of 1680 to 2000 W cm^{-2} (SPTP) frequently produced a bright echo at the beam focus. At 1200 W cm^{-2} , there was no echogenic feature on the image. When an echo did appear at the beam focus there were

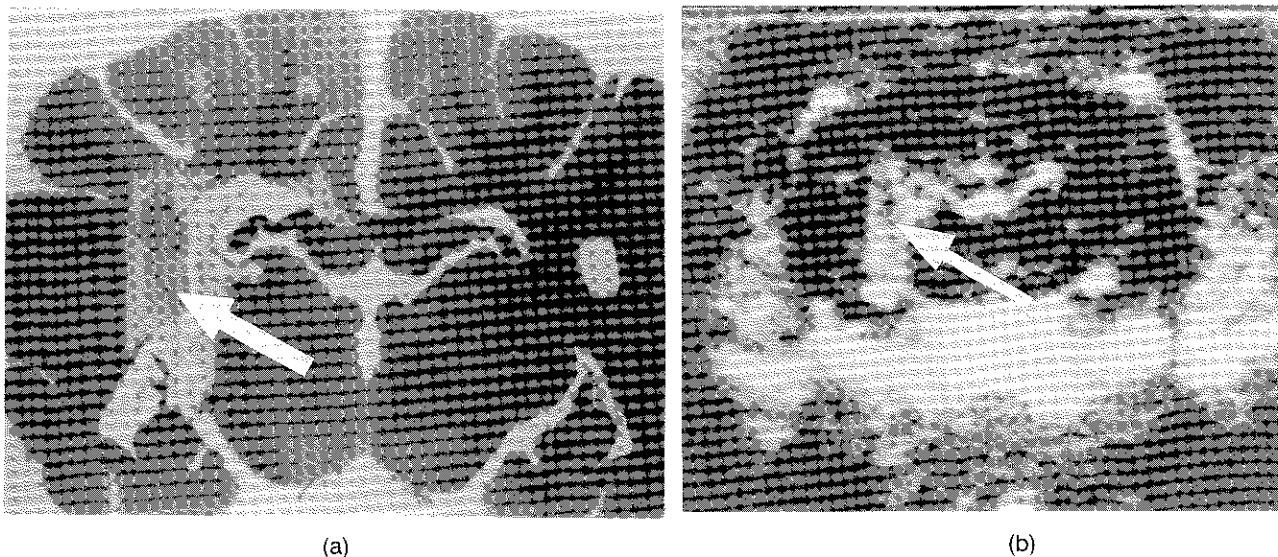


Fig. 4. (a) Histologically prepared coronal section showing area lesion in the dog brain. Lighter stained area on the left side of the figure. (b) Echogram showing the lesion site in coronal section at 3 weeks posttreatment. The animal was killed at 3 weeks and the slide shown in (a) was prepared. The echogram (b) is approximately two thirds the size of the histology presentation (a) as shown. The arrows point to the lesion site.

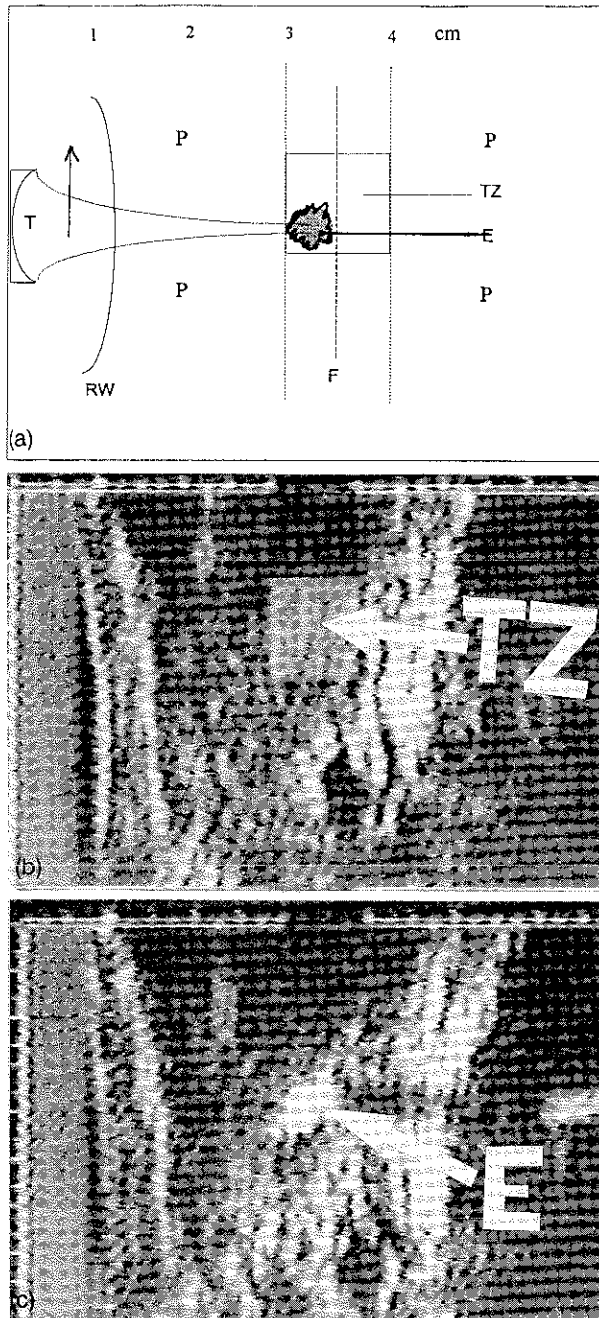


Fig. 5. (a) Schematic of arrangement. T—transducer, RW—rectal wall, P—prostate tissue, TZ—treatment zone box, F—center of focus of the beam, E—echogenic focus (gas phase). The arrow shows the direction of transducer movement of 2-mm steps. (b) Echogram before irradiation showing the TZ zone box. (c) Echogram after focal irradiation at one single site. The first bright thin echo 1 cm from the left of the echogram is the rectal wall echo.

no subsequent echoes appearing outside the primary focal site(s) (Fig. 5).

In the human clinical study of prostate treatment with the same system, there were focal site echoes

elicited in some cases at a site intensity of 1680 W cm^{-2} at 4 MHz. Once a focal site echo appeared it was frequently followed by a sequence of other echoes in the beam entry pathway on subsequent irradiations indicating a migration of microbubbles in the vascular system. The circulating microbubbles were apparently sources for cavitation events occurring in the sound field which in turn greatly expanded the number of microbubbles so that the events could be readily detected on the visualization scanning after each irradiation. The sequence of events can best be presented from a series of echograms taken during the course of treatment. All the echograms shown are linear scans of the prostate starting at the bladder neck and proceeding to the urethral exit. Figure 5 shows an echogram of the prostate before irradiation and an echo generated at the beam focus after a single-site irradiation. The follow-up scans occur at 2 s after the site is irradiated.

The sequence of echograms starting with Fig. 6a shows a composite echo in the focal zone of the transducer after four sites are irradiated (2 mm apart) in a linear displacement. The next site (site 5) was immediately followed by an extensive echo in front of the focal zone (Fig. 6b) and this echo produces some obscuring of the focal zone echo of Fig. 6a. After two more site irradiations in the linear displacement, the echo of Fig. 6b is further enlarged (Fig. 6c) and more obscuring of the Fig. 6a echo occurs. Figure 6d after one more site irradiation shows further obscuring. On the next and last site irradiation in this sequence a new echo appears (Fig. 6e) in front of the echo of Fig. 6d and the original focal zone echoes of Fig. 6a have virtually disappeared.

The typical appearance of the echo images for all laterally displaced linear site irradiations, after the previous sequence of events shown in Fig. 6 and associated scans, shows an essentially completely pervasive echo pattern in front of the focal zone completely obscuring tissue patterns beyond this broadly diffuse scattering region (Fig. 7).

DISCUSSION

Gallbladder and gallstones

Cavitation microbubbles using ultrasound and a chemical agent were deliberately induced in the gallbladder studies and found to be an effective accelerator of gallstone dissolution. The finding that the gallbladder could be completely eliminated due apparently to mucosal denuding, which must be totally ablated for this to happen, is a fortunate discovery. The reason for this total denuding is not altogether apparent. Denuding leading to gallbladder atrophy has not been reported in either clinical studies (May and Thistle 1986) or experimental animal studies (McGahan *et al.* 1988).

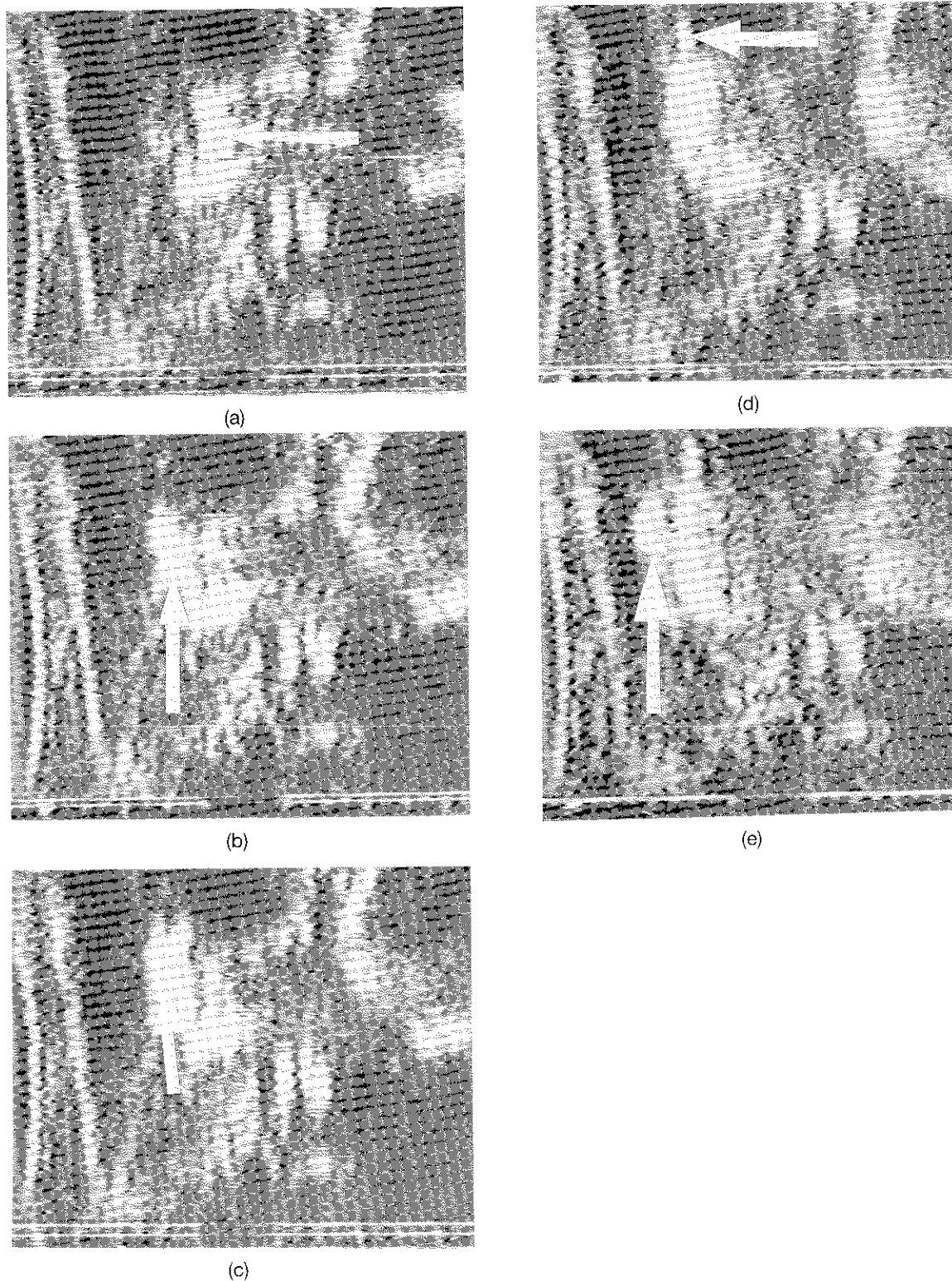


Fig. 6. Scans at various positions of the beam focus along a single linear path. (a) Scan after four sites were irradiated; the arrow indicates the bright echo which is in the very center of the TZ zone shown in Fig. 3. Note that the rectal wall is at the very left edge of the echogram (b) Scan after fifth irradiation; the arrow indicates a new echo appearing essentially 1 cm toward the rectal wall. (c) Scan after sixth irradiation; the arrow shows the increased longitudinal size of the echo. (d) Scan after seventh irradiation; the arrow indicates a further longitudinal extension of the echo. (e) Scan after eighth irradiation; the arrow indicates a new echo appearing essentially 1 cm toward the rectal wall from the echo seen on (d). See Fig. 5 for orientation.



Fig. 7. Scan at the beginning of the irradiation sequence in a position 2 mm lateral to the scan plane of Fig. 6. Fig. 5 schematic details the orientation. The first bright thin line echo 1 cm from the left edge is the rectal wall echo. The broad diffuse echo essentially shadowing the entire echogram is shown by the arrows.

Another feature was the ability to perform gallstone dissolution without gallbladder elimination, which was an effect obtained by reducing the sound intensity. Also, it was quite fortuitous that ultrasound intensities required for gallbladder atrophy could be coupled to the human skin surface without causing pain using degassed water direct coupling. This coupling scheme and gallbladder atrophy studies have not been implemented in the human. Additionally, the normal gallbladder anatomical placement permits the sound beam to cover the gallbladder without impinging on lung tissue which could be made hemorrhagic with such exposure (Child *et al.* 1990). The fact that other tissues and organs (stomach, intestines, skin and muscle) showed no gross evidence of damage at killing on either short- or long-term animals was extremely fortunate. With the 220-kHz frequency used the sound beam passing through the body had to be coupled to an exit absorber and this could be conveniently accomplished. The small human series (10 patients) provided no substantial information on gallstone erosion rates using ultrasound, because the protocol was written to call for ultrasound only if the MTBE dissolution of the gallstone procedure was too slow. This occurred in 2 of 10 patients but the ultrasound level which could be implemented (4 W cm^{-2}) appeared to be below that known to be more fully effective from the animal studies (3 W cm^{-2}). This initial series could be a guide for further clinical studies which might be extended to include gallbladder elimination. Certainly, attention to proper beam placement and direction is a necessary requirement in the use of this method.

Brain

Determination of the threshold intensity for cavitation microbubble production at 1 MHz in the dog brain is

essential information for any therapeutic use calling for volume lesion production in brain. Brain would appear to be one structure in which lesions outside focally selected sites would generally be undesirable so that volume lesion production would be accomplished by a multiplicity of thermally produced individual lesions. Since it appears that brain lesions would be produced in the frequency range of 1 to 4 MHz it is now possible to select the desired frequency and intensity to avoid cavitation leading to microbubble production. Other published data (Hynynen 1991) on dog thigh muscle would indicate a threshold at 1 MHz of somewhere between 500 and 900 W cm^{-2} (SPTP), which is in reasonable agreement with our value of 400 W cm^{-2} for brain at 1 MHz. Also, any extrapolation of dog thigh muscle data to 4 MHz would appear to indicate that a value of 1000 W cm^{-2} (SPTP) would be below the threshold for brain. Focal lesion production in all brains studied (cats, dogs, monkeys and man) indicate the same dosage requirements for thermal lesion production. This fact alone does not prove that the cavitation threshold and any subsequent microbubble transport will follow the same pattern, but it is an excellent starting point and the detection and determination of the cavitation threshold is readily accomplished with ultrasound scanning leading to avoidance of the phenomena and any serious consequences. In all cases involving focal lesion production at sites below the skin surface it is essential that cavitation at the skin surface be avoided. Previous studies indicate that this can be accomplished for the transcutaneous irradiation of brain. Since the cavitation threshold intensity *in vivo* has been shown in a number of cases to be a function of frequency, it is always desirable to work at the highest possible frequency consistent with tissue penetration capability and avoidance of cavitation at the skin entry site.

Prostate

Since the anticipated distance from the rectal wall to the deepest treatment site in the human prostate was 3 cm, the selection of 4 MHz as the transducer frequency for both visualization and lesioning was a good compromise. Use of this 4-MHz frequency meant that the cavitation threshold at the focal treatment site would probably be above 1000 W cm^{-2} (SPTP) (Fry and Meyers 1962; Hynynen 1991) and this proved to be true based on our indicators of ultrasound visualization and subsequent histology studies in the dog prostate. Since the proposed clinical treatment time was to be kept below 30 min the clinical need to build a large lesion volume within this time period pushed the focal intensity even higher, reaching beyond the cavitation threshold. The animal studies showed ultrasonic visualization of gas bubble generation as evidence by a

strong echogenic signal emanating from the focal site. In many cases, this echo persisted for up to the order of 1 min, but any presumed microbubble event did not seem to disturb subsequent focal lesioning placement nor did it lead to any ultrasound indicators or histological observation of lesions at off-focal sites.

In contrast to the animal studies the irradiation of human prostate at the intensity level of 1680 W cm^{-2} (SPTP) produced strong echogenic signals from the individual focal sites in a number of cases. When the heavy reflecting events occurred, they were frequently followed by further echogenic events at off-focal sites which have been interpreted as due to microbubbles migrating in the vascular system which, when irradiated with sound in the entry pathway, produce more microbubbles. These microbubbles could lead to lesion production at these new sites as observed in dog brain studies. The very extensive regions in the prostate, which show diffuse echogenic effects, appear to indicate a continuing proliferation of microbubble production at the very much reduced sound field intensities in the beam path. Histological verification of the lesioning consequences of these events in the human prostate is not available at present. It remains to be seen if the dog model can be manipulated to mimic the human condition. In any event, it seems apparent that volume lesion production in tissue using focal site intensities above the cavitation threshold may exhibit the stable bubble transport phenomena leading to possible lesioning at sites proximal to the focal seeding site. This effect, if properly monitored and controlled, could be of potential benefit in debulking of tissue when it may be warranted.

Due to the variety of circumstances surrounding the manner in which these studies were conducted the evidence for cavitation production is not the same in each case. Cavitation is presumed in the gallstone—gallbladder studies due to the *in vitro* findings at 190 psi in which gallstone erosion was suppressed at intensities that were the same as those used *in vivo*.

In the dog brain studies, the production of gross hemorrhagic lesions at tissue regions remote from the focal site(s) were presumed to be due to microbubble transport in the vascular system. The gross lesions observed subcortically (Fig. 3) were restricted to the side of the brain receiving the focal lesions. Since there is no crossover of the vascular circulation at the appropriate anatomical level in the brain there could be no bubble transport to the contralateral side, and hence, no grossly hemorrhagic lesions in subcortical regions receiving the same sound intensity as subcortical regions in the focally lesioned side of the brain. Additionally, reducing the focal sound intensity below 400 W cm^{-2} at 1 MHz completely eliminated the subcortical hemorrhagic effect.

In the human prostate, a similar microbubble transport process seems to occur. Echoes appear at the focal site on subsequent ultrasound scanning (within 2 s of irradiation) and these are presumably due to a vapor phase in the tissue, perhaps leading to a more volumetrically defined gas bubble. Starting from these focal sites a wave of diffuse echogenic sites appear in regions between the transducer and the focal center. These echogenic sites can become of such intensity as to prevent any visualization beyond their region. It is not yet known what role these echogenic sites play in tissue disruption since histology is not available in this situation.

In the dog prostate there are frequent occurrences of vapor phase echoes but a microbubble proliferation is not in evidence. The reason for this difference between the dog and man is not yet known.

CONCLUSIONS

Cavitation can be induced using ultrasound in fluid-filled body cavities with potential therapeutic possibilities and benefits. Careful attention to the handling of the various acoustic parameters and tissues exposed in the beam path demonstrate that this type of therapy can be safely applied as demonstrated in an appropriate animal model. In the complex process of applying non-invasive or relatively noninvasive methods to therapy it remains to be seen what role this technique, or similar procedures, will ultimately play.

In the situation involving production of volume lesions in tissue using a multiplicity of single-site focal lesions there are a number of potential choices available for therapeutic implementation. Depending on the circumstances, the entire regime can be conducted in the intensity range which produces thermal lesions without cavitation microbubble involvement. Once the cavitation threshold is exceeded, and depending on the local vascularity and other factors which at this stage are empirically derived, it is possible to produce large volume lesions without resorting to continuation of multiple, contiguous single focal site lesions as seen in the subcortical region in the dog brain. There appear to be at least two types of effects with vascular embedded microbubbles. One is the violent collapse type effect in which the blood vessels are disrupted and a tissue lesion produced due to loss of blood flow and mechanical damage. A second effect, seen perhaps for the first time in tissue, does not involve the circumstance where the microbubbles go through the collapse phase but stay at a size where substantially all the sound incident on the region could be trapped in the tissue volume leading to a tissue temperature rise which could provide nonhemorrhagic necrosis. The ability to control precisely these effects in tissue will

determine what role they might play in ablative therapy in the future.

Acknowledgements—We are very grateful to Drs. B. T. Burney, S. L. Griffith and T. D. Franklin, Jr. and G. Chua and R. Chua for their support during the gallstone dissolution and the brain tissue ablation projects.

REFERENCES

- Apfel, R. E. Acoustic cavitation prediction. *J. Acoust. Soc. Am.* 69:1624–1633; 1981.
- Benjamin, T. B.; Ellis, A. T. The collapse of cavitation bubbles and the pressures thereby produced against solid boundaries. *Philos. Trans. R. Soc. Lond. (Ser. A)* 260:221; 1966.
- Blake, F. G., Jr. The tensile strength of liquids: a review of the literature. Harvard University Acoustics Research Laboratory, Report NR-014-403; 1949.
- Bihrlé, R.; Foster, R. S.; Sanghvi, N. T.; Donohue, J. P.; Hood, P. J. High intensity focused ultrasound for the treatment of benign prostatic hyperplasia: early United States clinical experience. *J. Urol.* 151:1271–1275; 1994.
- Chapelon, J. Y.; Margonavi, J.; Theillière, Y.; Gorry, F.; Blanc, E.; Gelet, A. The effects of high energy focused ultrasound on kidney tissue in the rat and the dog. *Eur. Urol.* 22:147–152; 1992.
- Child, S. Z.; Carstensen, E. L.; Law, S. K. Effects of ultrasound on drosophila: III. Exposure of larvae to low-temporal-average-intensity, pulsed irradiation. *Ultrasound Med. Biol.* 7:167–173; 1981.
- Child, S. Z.; Hartman, C. L.; Schery, L. A.; Carstensen, E. L. Lung damage from exposure to pulsed ultrasound. *Ultrasound Med. Biol.* 16:817–825; 1990.
- Crum, L. A.; Fowlkes, J. B. Acoustic cavitation generated by microsecond pulses of ultrasound. *Nature* 319:52–54; 1986.
- Eller, A.; Flynn, H. G. Generation of subharmonic of order one half by bubbles in a sound field. *J. Acoust. Soc. Am.* 46:722–727; 1969.
- Esche, R. Investigation of vibratory cavitation in liquids. *Akust. Beih.* 4:208–218; 1952.
- Flynn, H. G. Cavitation dynamics. II. Free pulsations and models for cavitation bubbles. *J. Acoust. Soc. Am.* 58:1160–1170; 1975.
- Foster, R. S.; Bihrlé, R.; Sanghvi, N. T.; Fry, F.; Kopecky, K.; Regan, J.; Eble, J.; Hennige, C.; Hennige, L. V.; Donohue, J. P. Production of prostatic lesions in canines using transrectally administered high intensity focused ultrasound. *Eur. Urol.* 23:330–336; 1993.
- Fowlkes, J. B.; Irey, F. A.; Gardner, J. M.; Rubin, J. M.; Carson, P. L. New acoustic approaches to perfusion and other vascular dynamics. Abstract in program of the 127th Meeting of the Acoustic Society of America (#5). Vol. 95; 1994.
- Frizzell, L. A.; Lee, C. S.; Aschenbach, P. D.; Borrelli, M. J.; Morimoto, R. S.; Dunn, F. Involvement of ultrasonically induced cavitation in the production of hind limb paralysis of the mouse neonate. *J. Acoust. Soc. Am.* 74:1062–1065; 1983.
- Fry, F. J. Intense focused ultrasound in medicine. Some practical guiding physical principles from sound source to focal site in tissue. In: Marberger, M., ed. *Thermal tissue ablation*. *Eur. Urol.* 23(suppl. 1):2–7; 1993.
- Fry, W. J.; Barnard, J. W.; Fry, F. J.; Brennan, J. F. Ultrasonically produced localized selective lesions in the central nervous system. *Am. J. Phys. Med.* 34:413–423; 1955.
- Fry, F. J.; Burney, B. T.; Griffith, S. L.; Sanghvi, N. T.; Franklin, T. D. Ultrasound-enhanced cholelitholysis. *Radiology* 165(suppl.):311; 1987.
- Fry, W. J.; Dunn, F. Ultrasound: Analysis and experimental methods in biological research. In: Nastuck, W., ed. *Physical Techniques In Biomedical Research*, Vol. 4. New York: Academic Press; 1962:261–393.
- Fry, F. J.; Kossoff, G.; Eggleton, R. C.; Dunn, F. Threshold ultrasound dosages for structural changes in the mammalian brain. *J. Acoust. Soc. Am.* 48:1413–1417; 1970.
- Fry, W. J.; Meyers, R. Ultrasonic method of modifying brain structures. First International Symposium on Stereoccephalotomy, Philadelphia, PA, 1961. *Confin. Neurol.* 22:315–327; 1962.
- Fry, F. J.; Sanghvi, N. T.; Morris, R. F.; Smithson, S.; Atkinson, L.; Dines, K.; Franklin, T.; Hastings, J. A focused ultrasound system for tissue volume ablation in deep seated brain sites. *IEEE Ultrasonics Symp. Proc.* 2:1000–1004; 1986.
- Griffith, S. L.; Burney, B. T.; Fry, F. J.; Franklin, T. D. Experimental gallstone dissolution with methyl-tert-butyl ether (MTBE) and transcavitous ultrasound energy. *Invest. Radiol.* 25:146–152; 1990.
- Hynynen, K. The threshold for thermally significant cavitation in dog's thigh muscle *in vivo*. *Ultrasound Med. Biol.* 17:157–169; 1991.
- Jones, I. R.; Edwards, D. H. An experimental study of the forces generated by the collapse of transient cavities in water. *J. Fluid Mech.* 7:596–609; 1960.
- Lele, P. P. Cavitation and its effects on organized mammalian tissues. In: Fry, F., ed. *Ultrasound: its applications in medicine and biology (part II)*. Amsterdam: Elsevier; 1978:737–741.
- May, G. R.; Thistle, J. L. Percutaneous cholecystostomy for gallstone dissolution by methyl tert-butyl ether. *Radiology* 161(P):90; 1986.
- McGahan, J. P., et al. Dissolution of gallstones using methyl tertiary-butyl ether in an animal model. *Invest. Radiol.* 23:599–603; 1988.
- Neppiras, A. E. Subharmonic and other low-frequency emission from bubbles in sound-irradiated liquids. *Acoust. Soc. Am.* 46:587–601; 1968.
- Noltingk, B. E.; Neppiras, E. A. Cavitation produced by ultrasonics. *Proc. Phys. Soc. (London)* 63B:674–685; 1950.
- O'Brien, W. D. Jr.; Zachary, J. F. Comparison of mouse and rabbit lung damage exposure to 30 kHz ultrasound. *Ultrasound Med. Biol.* 20(3):299–307; 1994.
- Sanghvi, N. T.; Fry, F. J.; Burney, B. T.; Griffith, S. L.; Franklin, T. D.; Morris, R. F. A low frequency (220 kHz) ultrasound system for enhancement of gallstone dissolution. *IEEE Ultrason. Symp. Proc.* 3:1635–1638; 1990.
- Sanghvi, N. T.; Foster, R. S.; Fry, F. J.; Bihrlé, R.; Hennige, C.; Hennige, L. D. Ultrasound intracavity system for imaging, therapy planning and treatment of focal disease. *IEEE Ultrason. Symp. Proc.* 2:1249–1253; 1992.
- Sommer, F. G.; Pounds, D. Transient cavitation in tissues during ultrasonically induced hyperthermia. *Med. Phys.* 9:1–3; 1982.
- Tarantal, A. F.; Canfield, D. R. Ultrasound-induced lung hemorrhage in the monkey. *Ultrasound Med. Biol.* 20:65–72; 1994.
- ter Haar, G. R.; Daniels, S.; Eastaugh, K. C.; Hill, C. R. Ultrasonically induced cavitation *in vivo*. *Br. J. Cancer* 45(suppl. V):151–155; 1982.

